Modes of Grain Growth in Cold Rolled 3.25% Si–Fe and 3.25% Al–Fe Alloys

— A Proposal for Grain Growth by Analogy with Crystal Growth —

Hitoshi NAKAÉ*

(Received July 31, 1974)

Synopsis

The phenomena involved in the grain growth of cold rolled dilute alloys of iron were treated on the basis of an analogy with crystal growth. The migrating boundary is associated with the interface between the crystal and the medium from which the crystal grows. Thus, the deviation in composition from nominal one was expected in the regions on either side of the migrating boundary according to the mode of crystal growth and these regions are supposedly subjected to a phase transformation at the deviated compositions other than the nominal ones at ascending temperatures.

In 3.25% Si–Fe and 3.25% Al–Fe alloys, the influences on the grain growth were as follows.

1) the growth rate was retarded at the A_3 transformation corresponding to iron,

2) the growth of cube on edge texture was enhanced in Si–Fe alloy with sulfur addition at the point corresponding to the eutectic point of the S–Fe alloy system and

3) the growth of cube texture was enhanced at temperatures exceeding three eutectics in Si–Fe and along the solidus in Al–Fe alloy.

The development of cube texture in 3.50% Ge–Fe alloy and that of cube on edge texture in 3.25% Si–Fe alloy with small additions of aluminium or germanium were also ascribed to the above considerations.

I. Introductory

Among the many problems involved in the grain growth in cold rolled alloys to be solved, in the present paper those of dilute alloys of iron will be considered.

In 3.25% Si–Fe and 3.25% Al–Fe (Si–Fe and Al–Fe henceforth for brevity) alloys, which are noteworthy for their magnetic properties, the grain growth curves seem to be too complicated for the driving force based on the grain boundary energy formed during primary recrystallization. This is shown in the

* Department of Precision Engineering, Faculty of Engineering, Hokkaido University.

torque maximum curves, for example, of Si–Fe and Al–Fe alloys given in Fig. 1. The texture with an orientation of (110) [001] as the main component (cube on edge texture) develops in Si–Fe alloy[1] and that with an orientation of (100) [001] as the main component (cube texture) in Al–Fe alloy[2),3)] from similar weak textures with an orientation of (110) [001] as the main component of primary recrystallization.

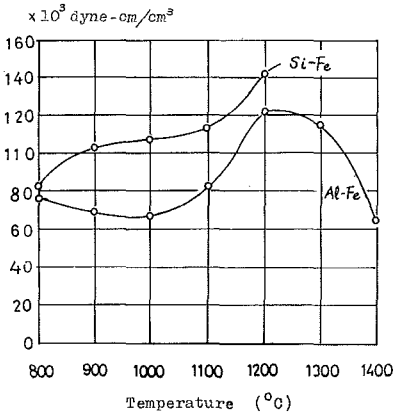

Fig. 1. Torque maximum vs annealing temperature on Si–Fe and Al–Fe alloys after author and Bozorth[2)] respectively.

The Si–Fe alloy has also noticeable properties where the texture with an orientation of (110) [001] as a component becomes obvious by small additions, amount of 1/10~1/100%, of some elements[4)~11)] and that with an orientation of (100) [001] at an annealing temperatures exceeding 1200°C[12)~14)].

The fact that these alloys with in common a weak texture of an orientation of (110) [001] as the main component happen to take a texture with an orientation of (100) [001] as the main component indicates that the other tendency surpasses or overtakes the proper tendency for growth.

Then, for the explanation of the development of cube texture in Al–Fe the contribution of aluminium nitride (AlN) has been proposed by Taguchi and Sakakura[15)] and for that in Si–Fe alloy surface energy difference by Walter and Dunn[16),17)] and for the enhanced development of cube on edge texture in Si–Fe alloy by a small addition of some elements was attributed to an inhibitory effect by May and Turnbull[9),10)].

The author has sought for an explanation with a consistency to cover all these phenomena and made a proposal that the grain growth in cold rolled alloys was carried by the mode of crystal growth from liquid e. g. solution growth or melt growth[18)] with reference to phase diagrams.

A mechanism will be proposed here which can meet the above requirements on the behaviors of grain growth with special regard to the effects of additions to iron.

II. Experimental

The alloy specimens were the same as those prepared in the papers elsewhere[3),11)] and were composed of materials with additions of 3.18~3.61% silicon and 3.17% aluminium to iron and those with a small addition of sulfur as listed in Table 1. In this experiment, 3.50% Ge–Fe alloy was also prepared as the reference material.

The details of the treatment of the alloys were also the same as in the papers above mentioned with a final thickness of 0.35 mm by cold reduction of about 75% after hot rolling.

TABLE 1 Chemical compositions of alloy specimens (wt %)

Alloy	Specimen No.	Si	Al	C	S	Mn	P	Bal.
Si-Fe	1S	3.61	—	0.005	0.007	Tr.	0.003	Fe
	2S	3.56	—	0.008	0.012	Tr.	0.002	Fe
	3S	3.18	—	0.002	0.120	0.06	0.002	Fe
Al-Fe	1A	0.01	3.17	0.007	0.004	—	0.002	Fe
	2A	0.01	3.17	0.009	0.060	—	0.002	Fe
	3A	0.04	3.17	0.300	0.148	—	0.002	Fe

* Data on specimen Nos. 2S and 2A have not practically cited in the results.

For the experiments a torque magnetometer, an electron microscope and an electron probe microanalyser (EPMA) were used.

III. Results and discussion

Among the factors contributing to a high concentration of impurities around a grain boundary, grain boundary migration is considered to be one of the most influential ones. The leading works on this theme have been givens by Cahn[19], and Lüke and Stübe[20]. The ultimate schematic diagram on the distribution of foreign atoms around the boundary in Fig. 2 (a) is compared with that of our proposal which obeys the modes of crystal growth[21] in Fig. 2 (b).

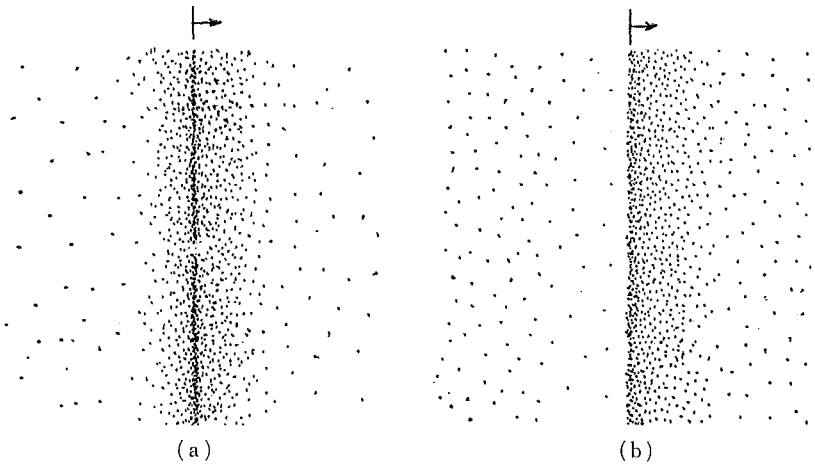

Fig. 2. Schema of foreign atom distributions around migrating boundaries, following ultimate concept so far (a) and that after crystal growth (b). Boundaries migrate toward →.

Here the basic consideration of the proposal is as follows. The migrating boundary leaves behind it a region free from foreign atoms and defects pushing them in front. The defects are dissipated during the process. Thus, both sides of the boundary show a sharp contrast in the concentrations of foreign

atoms. This situation is thermodynamically unstable and transient, and then both regions may be minute due to the high mobility of metallic atoms.

These two schematic diagrams signify substantially different effects on the grain boundary migration. The impurity distribution shown in Fig. 2 (a) will act only as a drag force against the migration of the boundary, whereas that in Fig. 2 (b) will build a potential to motivate the atom flow from one side to the another and also give a tendency in which the process continues in the same direction.

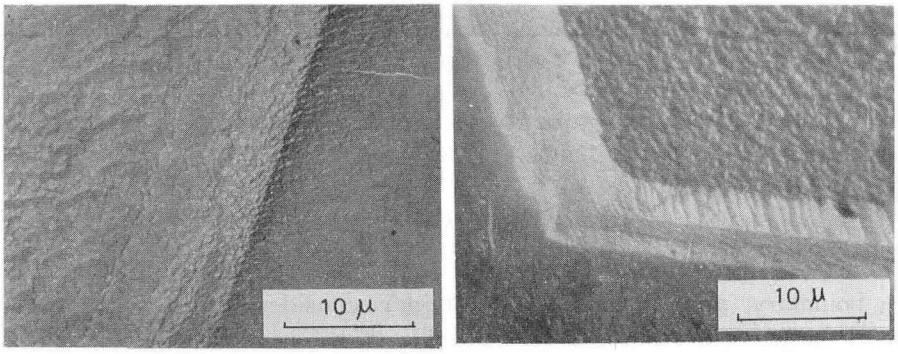

Si–Fe Al–Fe

Photo. 1. Electron microphotographs of grain boundaries using replica method on Si–Fe and Al–Fe alloys (Specimen Nos. 1S and 1A respectively) annealed at 900°C for 1 hr.

Electron microphotographs of specimens of Si–Fe and Al–Fe alloys without sulfur addition annealed at 900°C for 1 hr are given in Photo. 1. The regions around the boundaries are seen as a bright band divided into two parts by center lines and the widths measure about 10 micro-meters.

Although it is difficult to measure the exact momentary distribution of foreign atoms around the migrating boundaries, since the process is presumably transient, a diffractograph by EPMA may give some indications of deviations in compositions around the boundaries.

After microscopical observation, the specimens were indented at two points on the same sites across the boundary and buffed ; these were scanned by EPMA as shown in Fig. 3. The signs of increase or decrease of spreads in silicon and aluminium correspond to the respective decrease or increase in iron to some extent, and a pair of both signs is often found. It is worthy of note that the elements regarding alloying additions were measured across grain boundaries as well as those so-called impurities such as sulfur, phosphorous etc. and the pair of ±signs of spread corresponds to the proposed schematic diagram of foreign atom distribution around the migrating boundary in Fig. 2 (b).

When the temperature is elevated, the regions on either side of the migrating boundary may encounter the temperature of phase transformation corresponding to their deviated compositions other than the nominal ones (see Fig. 4). Here,

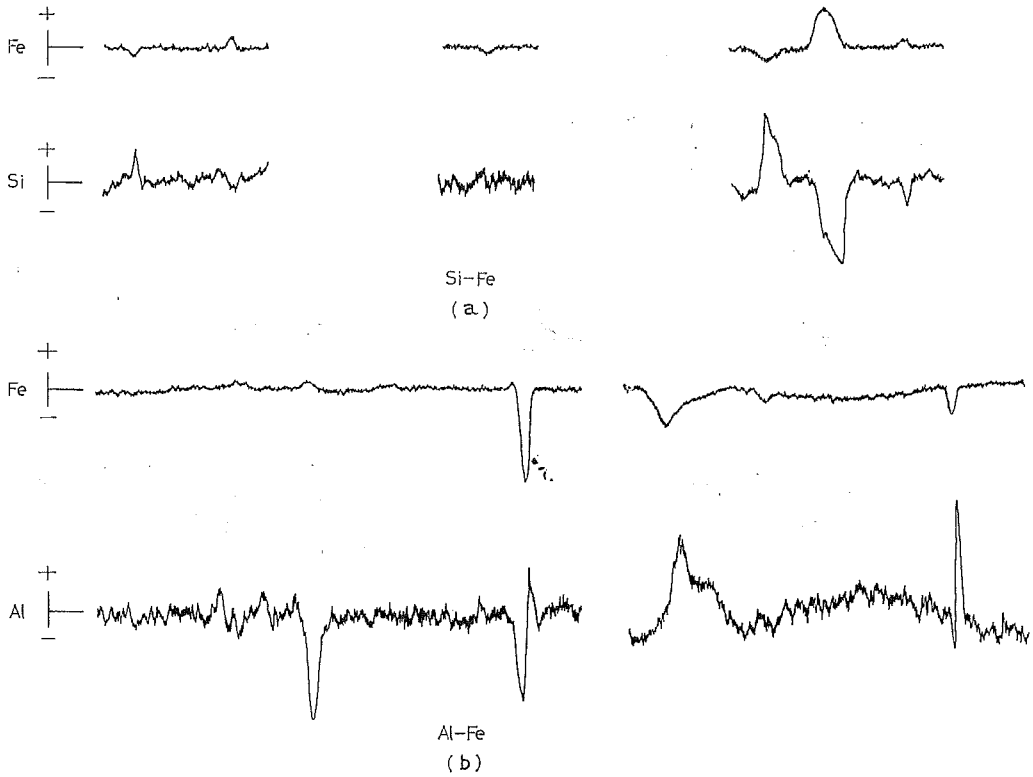

Fig. 3. EPMA diffractographs of spread of foreign atom distribution on Si and Al with Fe across boundaries in respective Si–Fe (Specimen No. 1S) and Al–Fe (Specimen No. 1A) alloys. + and − show respective increase and decrease from nominal distribution.

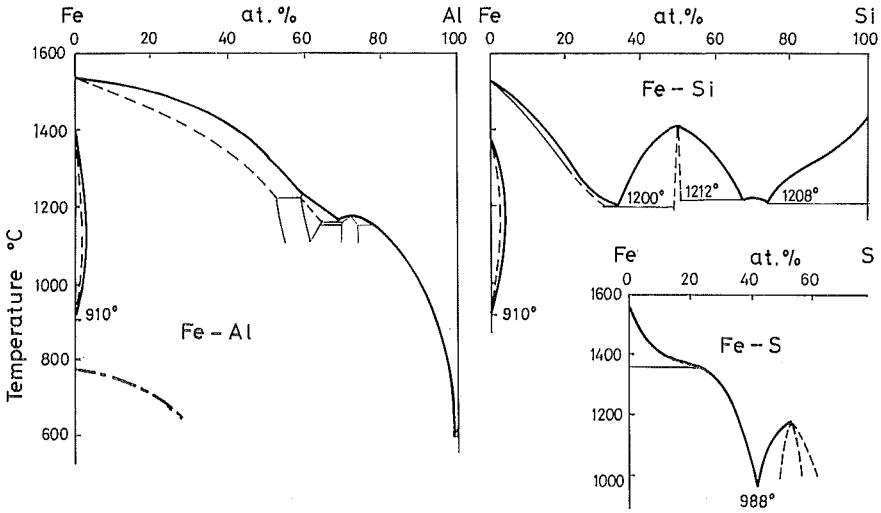

Fig. 4. Phase diagrams of Fe–Al, Fe–Si and Fe–S alloy systems.

the considerations on the relationship between the grain growth and the phase equilibrium will be henceforth discussed under the premise that each phase diagram of binary alloys cited here is not substantially changed even in the ternary systems consisting of silicon and sulfur with iron, and aluminium and sulfur with iron, since those of the ternary systems are not known as yet.

An approach to the phase equilibrium state was discussed tentatively at an ascending temperature based on a compromise between the process motivated by crystal growth and thermal fluctuations.

Thus, grain size vs temperature and torque maximum vs temperature are given in Fig. 5, in which the latter differs from that in Fig. 1 in the measured temperature intervals in particular, precise around the point of transformation.

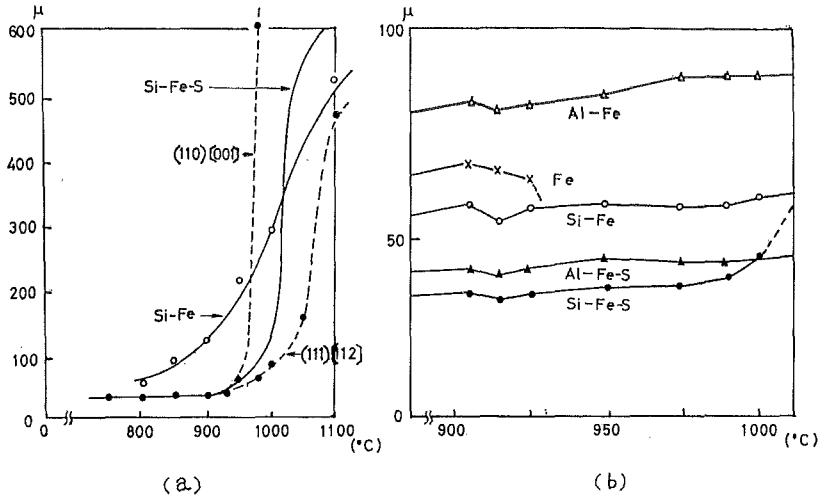

Fig. 5. Grain size vs temperature and torque maximum vs temperature on Si–Fe and Al–Fe alloys with and without sulfur additions. Grain size of Si–Fe alloy with sulfur addition is shown as decomposed in (110) [001] and (111) [11$\bar{2}$] components.

Specimen No. 1S -○-○-, No. 3S -●-●-, No. 1A -△-△-, No. 3A -▲-▲- and Fe -×-×-.

At first, the small drops at around 900°C are considered to be a process arising at the A_3 transformation in iron and a detailed explanation is presumably as follows.

The regions behind the migrating boundary may consist of regions gradually varying in concentration with foreign atoms as shown in Fig. 6. At ascending temperature, the boundary of γ phase region will shift toward point P from the A_3 point of iron, while the concentration of alloy at point P also moves backward toward P′ by thermal fluctuations, and then the transformation will virtually cease at a far lower temperature.

From the exact correspondence of the initial point of drops in alloys with that of pure iron, it may be surmized that a state of almost pure iron occurs in

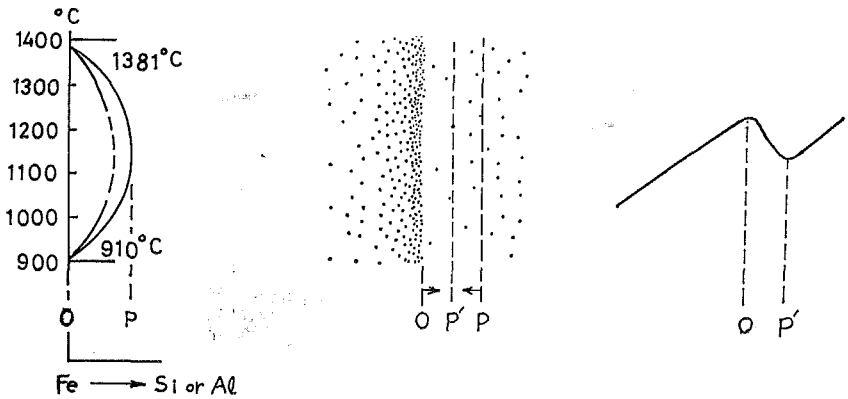

Fig. 6. Schema explaining boundary migration at around A_3 transformation.

the micro-regions just behind the migrating boundaries. This fact together with the diffractographs by EPMA in Fig. 3 seems to constitute influential evidence for the proposal that the grain boundary migration during grain growth is carried by the mode of crystal growth.

Then, if the region in front of the migrating boundary attains a liquidus or eutectic point corresponding to its deviated composition at ascending temperature, there may emerge a liquid phase along the front of the boundary which is distinguished from the solid boundary where no liquid phase is included in the boundary.

In a solid boundary, the mobility of atoms which proceeds the boundary migration would be rather slow, but if a liquid phase appears there can be expected some marked phenomena such as[21];

1) an acceleration of the growth of grains facing the liquid phase,
2) a preferential growth of grains oriented in a certain fashion and
3) origination of nuclei in a liquid phase.

Item 1) will due to a high potential built between the solid and liquid parts of regions along the boundary and a high mobility of atoms through the liquid, item 2) is the process observed in a dendritic growth in cast iron in which the direction and plane of growth are in pararell with the [100] direction and (100) plane, and item 3) is also the basic process seen in crystal growth as melt growth, solution growth or eutectic growth, in which the orientation of growing crystal is prescribed by certain external conditions. In cold rolled alloys, along the rolling direction and plane, (100) plane and [100] direction may align.

Among these three items, items 2) and 3) may contribute to the development of cube texture. Which one of these three items shows a preference in grain growth will depend on the conditions of the emerging liquid phase, mainly on the volume of the phase, and eventually on the amount of additions and the character of phase diagrams. This situation may be explained by the fact that the thin layer of liquid phase along the grain boundary may enhance the mobility

of atoms passing through it and the migration of boundary i. e. the grain growth may thus be enhanced. In this case, no other motivation surpasses the tendency so far and then the continued development of cube on edge texture is enhanced. This will be the case in sulfur addition, seen as an abrupt development of texture at about 960°C on grain size vs temperature and torque maximum vs temperature in Fig. 5 since a very small addition of sulfur and sharp cusped single eutectic built with iron could only provide a thin layer of liquid.

Photo. 2 shows the structure of Si–Fe alloy with sulfur addition (Specimen No. 3S) annealed at 1000°C for 1 hr. The configurations in the figure can not be expected to enhance the tendency of grain growth toward minimizing the grain boundary energy i. e. grain boundary length in the figure. According to Ainslie and Seybolt[8], the sulfur in this alloy exceeded the solubility limit even at this temperature and thus the existence of a second phase i. e. liquid phase may be surmized. The fact that the grain growth is active at this temperature is due to the liquid phase.

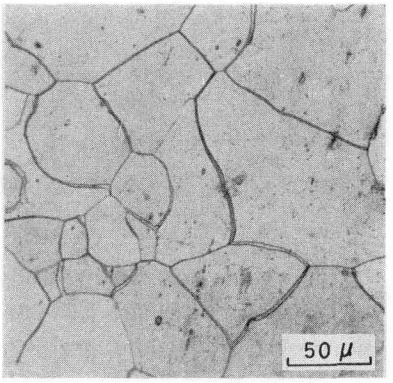

Photo. 2. Optical micrograph on Si–S–Fe (Specimen No. 3S) annealed at 1000°C for 1 hr.

Increasing liquid phases can not however, always give enhancement of boundary migration. But when a liquid phase attains an appreciable amount, a primary nucleous may be initiated and this tendency will be enhanced with the increasing liquid phase.

The phase diagrams of molybdenum and germanium with iron are shown in Fig. 7. These alloys can undergo a development of cube grain along the

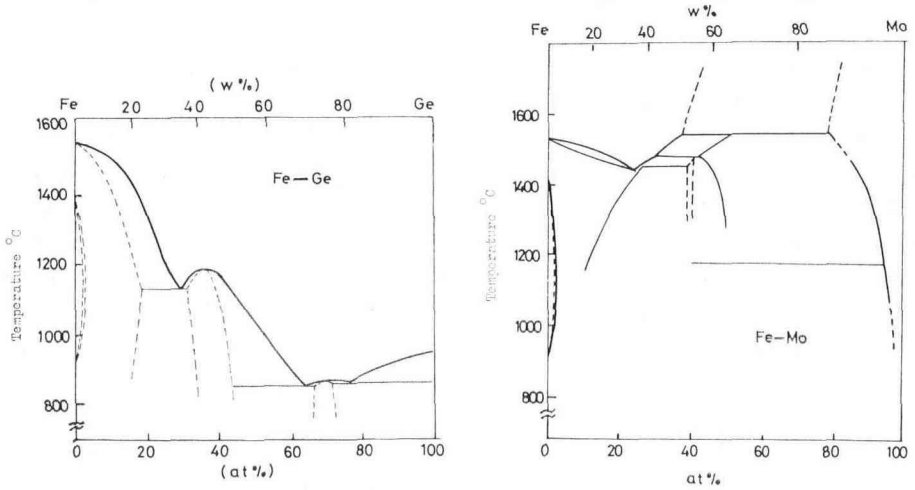

Fig. 7. Phase diagrams of Mo–Fe and Ge–Fe alloy systems.

solidus in an analogous fashion with the Al–Fe alloy and may show some anomaly at the eutectics. Mo–Fe alloy is known to develop cube texture[14]. The torque maximum and torque ratio vs temperatures of 3.50% Ge–Fe alloy are shown in Fig. 8 (a) and (b). The torque ratios of 0.7~0.8 mean that the texture embodies much cube component.

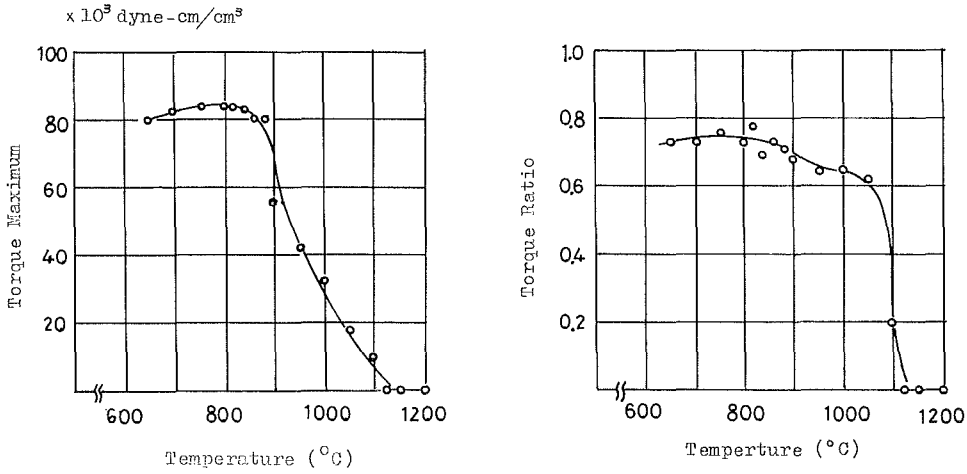

Fig. 8. Torque maximum vs temperature (a) and torque ratio vs temperature (b) on 3.50% Ge–Fe alloy annealed at heating rate 2°C/min.

In Si–Fe at annealing temperatures exceeding 1200°C, three eutectics at 1200, 1208 and 1212°C will cooperate additively and the cube tuxture will show an enhanced development.

According to the above considerations, it is worthy of note that an addition of the same elements can enhance the development of either cube on edge texture or cube texture. A fractional additions of a percent of aluminium[22] and germanium[23] to 3.25% Si–Fe developed cube on edge texture. In these cases also, the configurations in primary recrystallization texture such as group formation among similarly oriented grains and foreign atom concentrations around boundaries with high misfit angles may be satisfied[11].

It is also of interest and plausible that the growth of (100) [001] component is enhanced with increasing aluminium additions by replacing the silicon in 3.25% Si–Fe retaining the total amount of alloying additions constant[24].

The discussions on phase equilibrium held heretofore were based on the fact that equilibriums approaching in micro-regions such as grain boundary, surface etc, essentially differed from that in bulk regions and are carried by a compromise between the migrating boundary to bring the compositional deviations and the thermal fluctuations to bring it back.

As for the influence of the process, although it arises in a minute region, the results brought about by the process can by no means be meager, since the regions migrate through the matrix grains following the migrating boundary and hence the effect is integrated. Lastly, an additional argument will be given.

It will be more convincing if the primary nucleous with (100) [001] orientation emerging in a liquid phase can contribute to the formation of cube texture in Si–Fe and Al–Fe alloys during grain growth rather than that some preferred conditions to the enhanced growth of (100) [001] component embodied in the primary recrystallization texture. The proposals based on the latter[15)~17)] will set forth some problems such as the primary recrystallization texture must contain far more (100) [001] grains with the least orientation fluctuations. This condition however has never been satisfied.

IV. Summary

The grain growth in cold rolled dilute alloys of iron was discussed on the assumption that the growing grain is analogous to a growing crystal from liquid e.g. solution growth and the grain boundary to an interface between a crystal and solution. Thus, the compositional deviation in the regions on either side of the interface was associated to the character of the entire range of phase diagrams of the alloy system.

The grain growth behavior in Si–Fe and Al–Fe alloys with and without sulfur addition may be summarised as ;

The growth rate was influenced by the characteristic points in a phase diagram in such a way that the retardation due to A_3 transformation in iron and the acceleration due to the eutectic of the S–Fe alloy system.

The developments of cube on edge texture and cube texture were ascribed to the emergence of liquid phase as : the former to the atomic diffusion through liquid phase and the latter to the intiation of a primary nucleous in the liquid phase.

Acknowledgement

The author wishes to express his profound gratitude to Profs. M. Pope of New York University, P. Coulomb of Université Paul Sabatier, Y. Iwama of Nagoya University, M. Takahashi of Tohoku University and K. Nishida of Hokkaido University for providing suggestive discussions and also to Dr. K. Tagashira for offering data.

References

1) R. G. Aspden, J. A. Berger and R. S. Mateer : Trans. AIME, **215** (1959), 251.
2) R. M. Bozorth : *Ferromagnetism*, Van Nostrand Comp., New York, **58** (1953), 219.
3) H. Nakaé and N. Goshi : Trans. JIM, **15** (1974), 295.
4) H. Fiedler : Trans. AIME, **221** (1961), 1201.
5) H. Fielder : *Ibid*, **227** (1963), 776.
6) H. Fiedler : J. Appl. Phys., **29** (1958), 361.
7) E. W. Walter and J. Howard : J. Iron and Steel Inst., **194** (1960), 96.
8) N. G. Ainslie and U. Seybolt : *Ibid*, **194** (1960), 341.
9) J. May and D. Turnbull : Trans. AIME, **212** (1958), 769.
10) J. May and D. Turnbull : J. Appl. Phys., **30** (1959), 210.

11) H. Nakaé and K. Tagashira: Trans. JIM, **14** (1973), 15.
12) F. Assmus, K. Detert and G. Ibe: Z. Metallk., **48** (1957), 344.
13) G. Wiener: J.Appl. Phys., **35** (1964), 856.
14) G. Wiener, P. A. Albert, R. H. Trapp and M. F. Littmann: *Ibid*, **29** (1958), 366.
15) S. Taguchi and A. Sakakura: Acta Met., **14** (1966). 405.
16) J. L. Walter and C. G. Dunn: Trans. AIME, **215** (1959), 465.
17) J. L. Walter and C. G. Dunn: Acta Met., **8** (1960), 497.
18) H. Nakaé and N. Goshi: Memoirs of Faculty of Engineering, Hokkaido Univ., **13** (1974), 297.
19) J. W. Cahn: Acta Met., **10** (1962), 789.
20) K. Lüke and H. P. Stübe: *Recovery and Recrystallization of Metals*, Interscience, New York (1963), 171.
21) See for example: A. VanHook: *Crystallization*, Chapman and Hall Ltd., London (1965), or B. R. Pamplin: *Crystal Growth*, Pergamon Press, Oxford (1974).
22) S. Taguchi: Nihon Kinzoku Gakkai Kaiho, **13** (1974), 49 (in Japanese).
23) H. Hakaé: Unpublished data.
24) I. Gokyu, H. Abe, T. Hashida and S. Takahashi: J. JIM, **25** (1961), 712 (in Japanese).